RESEARCH ARTICLE

INTERNATIONAL MICROBIOLOGY

Characterization of the promoter region of *ftsZ* from *Corynebacterium glutamicum* and controlled overexpression of FtsZ

Michal Letek,[1] Efrén Ordóñez,[1] María Fiuza,[1] Pilar Honrubia-Marcos,[1¶] José Vaquera,[2] José A. Gil,[1]* Luís M. Mateos[1]

[1]Department of Molecular Biology, Area of Microbiology, Faculty of Biology, University of León, Spain. [2]Department of Molecular Biology, Area of Cellular Biology, Faculty of Biology, University of León, Spain

Summary. Of the five promoters detected for the *ftsZ* gene in *Corynebacterium glutamicum*, three were located within the coding region of the upstream *ftsQ* gene and two within the intergenic *ftsQ-ftsZ* region. The most distant *ftsZ* promoter showed activity in *Escherichia coli* and controlled high-level transcriptional expression of *ftsZ* in *C. glutamicum*. Quantitative Western blotting showed that all five promoters were active during the exponential growth phase and down-regulated during stationary phase. This tightly controlled expression of *ftsZ* in *C. glutamicum* indicated that small changes in the amount of FtsZ protein strongly affect bacterial cell viability. The controlled overexpression of *ftsZ* in *C. glutamicum*, using the promoter of the *gntK* gene (P*gntK*), resulted in approximately 5-fold overproduction of FtsZ, an increase in cell diameter, and a highly variable localization of the protein as spirals or tangles throughout the cell. These results suggest that the intracellular concentration of FtsZ is critical for productive septum formation in *C. glutamicum*. Our observations provide insight into the mechanisms used by the coryneform group, which lacks actin homologs and many regulators of cell division, to control cell morphology. [**Int Microbiol** 2007; 10(4): 271-282]

Key words: *Corynebacterium glutamicum* · *ftsZ* gene · *ftsZ* promoters · overexpression · rapid amplification of cDNA ends (RACE)

Introduction

FtsZ, a tubulin homolog, is considered the core of the cell-division process in most bacteria and archea [17,31]. FtsZ polymerizes to form a ring-like structure at mid-cell, recruits a variable number of proteins, and has been proposed to generate the constriction force required for cell division [9]. Small variations in the protein's ability to assemble strongly reduce bacterial cell viability by abolishing the cell-division process [41]. Consequently, FtsZ has been the subject of many studies aimed at developing new antibiotics [21,53]. The existence of different promoter regions for *ftsZ* was also described in *Escherichia coli*, in which at least two promoters lie in the upstream *ftsA* gene [12,14], and in *Streptomyces coelicolor*, which contains three putative *ftsZ* promoters in the *ftsQ-ftsZ* intergenic region [13].

To obtain symmetrical daughter cells, cell division in bacteria is tightly controlled by several spatial and temporal regulators; of these, the nucleoid occlusion and *min* systems are the most well-studied [48]. Nucleoid occlusion inhibits the assembly of FtsZ in the presence of DNA [57], whereas the *min* system blocks FtsZ assembly at the cell poles [48]. The combined effect of these two systems leaves the mid-cell, after nucleoid segregation, as the unique possible place for Z-ring formation in bacteria [9].

*Corresponding author: J.A. Gil
Departamento de Biología Molecular, Área de Microbiología
Facultad de Biología, Universidad de León
24071 León, Spain
Tel. +34-987291503. Fax +34-987291479
E-mail: jagils@unileon.es

[¶]Current address: Norel & Nature, Industrial Park of Vilecha, Onzonilla, León, Spain

Control of the FtsZ concentration may be another regulatory mechanism of cell division, although a general cell-cycle regulatory protein has been found only in *Caulobacter crescentus* [25]. Lower amounts of FtsZ, inhibition of FtsZ assembly, or malfunction of the protein cause a filamentous cell morphology in *E. coli* [3,5]. Concentrations of FtsZ higher than wild-type levels result in the appearance of polar Z-rings and asymmetric cell division, both in *Bacillus subtilis* and *E. coli* [55,56]. These clear effects on cell morphology suggest that the levels of FtsZ are tightly controlled in bacterial cells, a conclusion supported by the complexity of *ftsZ* gene transcription in different bacteria [12–14,16,42].

Corynebacterium is an important genus of the gram-positive actinobacteria group and certain species are of industrial and medical interest [28,37,51]. In *C. glutamicum*, the absence of actin homologs and of positive and negative regulators of cell division prompted us to carry out a detailed analysis of the transcriptional regulation of the bacterium's *ftsZ* gene (*ftsZ$_{CG}$*), by characterizing its promoters, and to study the effects of the modulated expression of FtsZ$_{CG}$ (using different promoters) in this species. In an earlier study, primer-extension analysis localized two promoters for *ftsZ$_{CG}$*, one in the intergenic *ftsZ-ftsQ* region and the other in the coding sequence of *ftsQ* [19]. In addition, we examined the ability of FtsZ$_{CG}$ to polymerize in *E. coli*, a bacterium that presents a model of cell division with many similarities to *C. glutamicum,* but also profound differences.

Materials and methods

Bacterial strains, plasmids, and culture conditions. The bacterial strains and plasmids used in this study are described in Table 1. *E. coli* cells were grown in Luria broth or Luria agar [18] at 37ºC with aeration. Corynebacterial strains were grown at 30ºC in trypticase soy broth from Oxoid (TSB, complex medium without glucose), TSA (TSB supplemented with 2% agar), or minimal medium for corynebacteria (MMC) [24]. To control expression of the promoter P*gntK*, MMC was supplemented with different sugars (up to 4%): gluconate (the lowest repression conditions), glucose (intermediate repression), fructose (high repression), or sucrose (the highest repression). When required, kanamycin (50 µg/ml for *E. coli*; 12.5 µg/ml for corynebacteria) and ampicillin (100 µg/ml for *E. coli*) were added to the culture media.

Nucleic-acid isolation and manipulation. Plasmid DNA was isolated from *E. coli* using the "Wizard® *Plus* SV Minipreps" from Promega. *E. coli* cells were transformed by the method of Hanahan [18]. DNA fragments were purifed using the "Wizard® SV Gel and PCR Clean-up System" from Promega. Restriction enzymes were purchased from MBI Fermentas and New England Biolabs. Plasmids from *E. coli* were mobilized into coryneform strains as described previously [36]. Total DNA from corynebacteria was isolated using the Kirby method described for *Streptomyces* [26], except that the cells were treated with lysozyme at 30ºC for 4 h. Samples of total DNA from *C. glutamicum* strains were used for PCR amplification with the primers described in Table 2. The correct chromosomal gene disposition in *C. glutamicum* KF was confirmed by PCR and Southern-blotting. For the latter, samples of total DNA were digested with restriction enzymes and loaded on agarose gels; the samples were transferred to nylon membranes and hybridized with the entire PCR-amplified *ftsZ* gene (labeled with digoxigenin; Roche) according to the manufacturer's instructions and conventional protocols.

RNA was isolated from *C. glutamicum* ATCC 13869 at the exponential growth phase using the RNeasy commercial kit (Qiagen). Primer extension experiments were performed according to the method of Kainz and Robert [23] using two synthetic primers (Pext-1 and Pext-2; Table 2). Rapid amplification of cDNA ends (RACE)-PCR experiments were carried out according to the "5′/3′ RACE Kit, 2nd Generation" protocol (Roche). In order to identify promoters located upstream from the *ftsZ* gene, 2 µg of total RNA and primer raceZ1 (Table 2) were used in the assay to generate single-stranded cDNA. A homopolymeric adenine-tail (A-tail) was added to the 3′-end of the purified cDNA preparation using terminal transferase, and the dA-tailed-cDNA was used in two further PCR amplification steps, the first with the primer pair dT/raceZ2 (Table 2). The amplified DNA product and the primer pair dT/raceZ3 were then used in the second round of PCR amplification (Table 2). The amplified fragments were cloned into pGEM-TEasy vector (Table 1), which makes use of the T-A cloning technique, and used to transform *E. coli* TOP10. Five plasmids isolated from different clones were sequenced for each amplified fragment.

Plasmid constructions. Promoter probe plasmids containing DNA regions immediately upstream from *ftsZ$_{CG}$* were constructed to quantify promoter strength. DNA fragments were PCR-amplified using total DNA from *C. glutamicum* ATCC 13869 and primers PftsZ1A/1B/2A/2B/3A/3B in different combinations (Table 2). The amplified fragments were digested with the indicated restriction enzymes (Table 2) and ligated to the *E. coli* promoter probe vector pJMFA24, which had been digested with *Bam*HI (Table 1), yielding plasmids of the series pJZ1/2/3/12/23/123 (Table 1). Promoter regions P*ftsZ1/2/3/12/23/123* were, respectively, isolated from plasmids pJZ1/2/3/12/23/123 by *Eco*RI-*Nde*I digestion, and further subcloned into the bifunctional *E. coli*-*C. glutamicum* promoter probe plasmid pEGFP (Table 1) by P*kan* promoter exchange, generating plasmids of the series pEGZ1/2/3/12/23/123 (Table 1).

The presence of the unique *Nde*I target in plasmids pEGZ123, pEGFP-MK, or pEAG6 (Table 1) allowed us to study expression of the gene fusion *ftsZ-egfp2* (*egfp2*, [49]) under the control of the promoter P*ftsZ123* (pEGZ123), P*gntK* (pEGFP-MK), or P*div* (pEGFP-MK). The 1.3-kb *ftsZ* gene was PCR-amplified from *C. glutamicum* 13869 using the primer pair ftsZ1/2 (Table 2) and the band was digested with *Nde*I. This band was further subcloned into the *Nde*I-digested plasmids pEGZ123, pEGFP-MK, and pEAG6 (Table 1, Fig. 1C), yielding plasmids pEGZ, pEKFG, and pEAG7E (Table 1), which contained the *ftsZ-egfp2* translational fusion under the control of P*ftsZ123*, P*gntK*, or P*div*, respectively.

To overexpress the *ftsZ$_{CG}$* gene without the *egfp2* fusion in *C. glutamicum*, *ftsZ$_{CG}$* was PCR-amplified (in this case including the stop codon; see Table 2) fused to the promoter P*gntK* or P*div*, using plasmids pEKFG or pEAG7E and primer pairs PgntK/ftsZ3 and Pdiv/ftsZ3 for the respective amplifications. PCR products of the expected sizes were subcloned into the EcoRV-digested pECM2 plasmid (Table 1), yielding plasmids pEKF (P*gntK-ftsZ$_{CG}$*) and pEAG7 (P*div-ftsZ$_{CG}$*).

To control the expression of *ftsZ$_{CG}$* as a single copy on the chromosome, the suicide mobilizable plasmid pKKF was designed to disrupt the chromosomal copy of the original gene and insert a new functional copy of *ftsZ$_{CG}$*, but in this case under the control of the P*gntK* promoter. Plasmid pKKF (P*gntK-ΔftsZ$_{CG}$*) was achieved by subcloning the 789-bp 5′-region of *ftsZ$_{CG}$* (which encodes the first 263 amino acids of FtsZ$_{CG}$), fusion to the P*gntK* promoter (obtained by *Xba*I-*Bam*HI digestion of plasmid pEKFG), blunting by Klenow, and ligation to the *Sma*I site of pK18mob (Table 1); only the orientation contrary to P*lac* was used.

To express *ftsZ$_{CG}$* fused to *gfp* in *E. coli*, the former was PCR-amplified using the primer pair ftsZ4/5 (Table 2). A PCR product of the expected size was subcloned into the *Hin*dIII-*Xba*I-digested plasmid pGFPuv, yielding plasmid pZGFP (P*lac-ftsZ$_{CG}$-gfp*) (Table 1).

Sequencing and DNA analysis. DNA sequencing was carried out by the dideoxy nucleotide chain-termination method of Sanger et al. [44].

Table 1. Bacterial strains and plasmids used in this work

Strain or plasmid	Relevant genotype or description	Source or Reference
Strain		
E. coli TOP10	F⁻ *mcr*A Δ(*mrr-hsd*RMS-*mcr*BC) φ80*lacZ*ΔM15 Δ*lacX74 deoR recA1 araD139* Δ(*ara-leu*)7697 *galU galK rpsL endA1 nupG*; used for general cloning	Invitrogen
E. coli HB101	F-Δ(*gpt-proA*)62 *leuB*6 *supE*44 *ara*-14 *galK*2 *lacY*1 Δ(*mcrC-mrr*) *rpsL*20 *xyl*-5 *mtl*-1 *recA13 thi*-1; used for general cloning	Promega
E. coli S17-1	Mobilizing donor strain, *pro recA*, which has a RP4 derivative integrated into the chromosome.	[46]
C. glutamicum ATCC 13869	Wild type	ATCC
C. glutamicum R31	*C. glutamicum* ATCC 13869 derivative, with improved efficiency of DNA uptake-stability and used as recipient in conjugations	[45]
C. glutamicum KF	*C. glutamicum* R31 derivative containing a complete copy of *ftsZ*$_{CG}$ under the control of P*gntK* obtained by integration of plasmid pKKF	This work
Plasmid		
pECM2	Mobilizable plasmid capable of replicating in *E. coli* and *C. glutamicum*; *kan* and *cat*	[22]
pEAG6	pECM2 derivative containing *egfp2* under the control of the *divIVA* promoter (P*div-egfp2*); *kan*	Letek et al. submitted
pEAG7E	pEAG6 derivative containing the *ftsZ*$_{CG}$-*egfp2* cassette under the control of P*div*; *kan*	This work
pEAG7	pEM2 derivative containing the *ftsZ*$_{CG}$ gene under the control of *divIVA* promoter (P*div- ftsZ*$_{CG}$); *kan*	This work
pEGFP	pEM2 derivative containing *egfp2* under the control of the P*kan* and flanked by transcriptional terminators T1 and T2; *kan*	[29]
pEGFP-MK	pEGFP derivative containing *egfp2* under the control of the 250 bp gluconate kinase promoter (P*gntK-egfp2*); *kan*	[29]
pEGNC	pEGFP derivative vector containing the promoter-less *egfp2* gene; *kan*	[29]
pEGZ	pEGZ123 derivative containing the *ftsZ*$_{CG}$-*egfp2* cassette under the control of P*ftsZ123*; *kan*	This work
pEGZ1	pEGFP derivative obtained by exchange of the P*kan* by the P*ftsZ1* promoter region; *kan*	This work
pEGZ12	pEGFP derivative obtained by exchange of the P*kan* by the P*ftsZ12* promoter region; *kan*	This work
pEGZ123	pEGFP derivative obtained by exchange of the P*kan* by the P*ftsZ123* promoter region; *kan*	This work
pEGZ2	pEGFP derivative obtained by exchange of the P*kan* by the P*ftsZ2* promoter region; *kan*	This work
pEGZ23	pEGFP derivative obtained by exchange of the P*kan* by the P*ftsZ23* promoter region; *kan*	This work
pEGZ3	pEGFP derivative obtained by exchange of the P*kan* by the P*ftsZ3* promoter region; *kan*	This work
pEKF	pEM2 derivative containing the *ftsZ*$_{CG}$ gene under the control of P*gntK*; *kan*	This work
pEKFG	pEGFP-MK derivative containing the *ftsZ*$_{CG}$-*egfp2* cassette under the control of P*gntK*; *kan*	This work
pGEM-TEasy	Vector used to clone PCR amplified products using Taq enzyme; *bla*	Promega
pJMFA24	*E. coli* promoter-probe vector containing the promoter-less *kan* gen as reporter; *bla*	[29]
pJZ1	pJMFA24 derivative containing the promoter region P*ftsZ1*; *bla*	This work
pJZ1123	pJMFA24 derivative containing the promoter region P*ftsZ123*; *bla*	This work
pJZ12	pJMFA24 derivative containing the promoter region P*ftsZ12*; *bla*	This work
pJZ2	pJMFA24 derivative containing the promoter region P*ftsZ2*; *bla*	This work
pJZ23	pJMFA24 derivative containing the promoter region P*ftsZ23*; *bla*	This work
pJZ3	pJMFA24 derivative containing the promoter region P*ftsZ3*; *bla*	This work

Table 1—*Continued*

Strain or plasmid	Relevant genotype or description	Source or Reference
Plasmid		
pK18mob	*E. coli* mobilizable plasmid; *kan*	[47]
pKKF	pK18mob derivative containing the 5′-end of the *C. glutamicum ftsZ$_{CG}$* gene under the control of the gntK promoter (P*gntK*-Δ*ftsZ$_{CG}$*) and used as suicide vector in corynebacteria; *kan*	This work
pGFPuv	*E. coli* pUC19 derivative Plasmid containing the *gfp* gene under the control of lactose promoter (P*lac*); *bla*	Clontech
pZGFP	pGFPuv derivative containing *ftsZ$_{CG}$*-*gfp* cassette under the control of *Plac*; *bla*	This work

ATCC, American Type Culture Collection; *kan*, *cat* and *bla* are kanamycin, cloramphenicol, and ampicillin resistance genes respectively; *gfp*, green fluorescent protein; *egfp2*, enhanced green fluorescent protein.

Computer analysis was performed with DNASTAR (DNAstar, London, UK), database similarity searches were done at the BLAST and FASTA public servers (NCBI, Bethesda, MD, USA), and multiple alignments of sequences using CLUSTAL W (EBI, Hinxton Hall, UK). Plasmid constructions were confirmed to be correct by sequencing.

Protein isolation and manipulation. *C. glutamicum* cells were disrupted using Fast PROTEIN Blue Lysing Matrix (Qbiogene, Carlsbad, CA, USA) and the BIO101 Thermo Savant FastPrep FP120 (Qbiogene Inc.). Following the recommendations of the manufacturer, 10 ml of cell culture at the desired optical density (OD$_{600}$) were pelleted and resuspended in 600 µl of phosphate-buffered saline (PBS). The suspension was homogenized in ice-cooled tubes for two periods of 20 s at a power setting of 6.0, with a 5-min interval. Cell debris and lysing matrix were removed by centrifugation at 10,000 ×*g* for 1 min at 4ºC, and supernatants were used as cell extracts.

The amount of protein was quantified as previously described [4]. Sodium dodecyl sulfate polyacrylamide gel electrophoresis (SDS-PAGE) of cell extracts from the different microorganisms was carried out essentially as described [27]. Electrophoresis was performed at room temperature in a vertical slab gel (170 × 130 × 1.5 mm) using 10% (w/v) polyacrylamide at running conditions of 100 V and 60 mA. After electrophoresis, the proteins were stained with Coomassie blue or electroblotted onto polyvinylidene difluoride (PVDF) membranes (Millipore) and immunostained with 1:10,000 dilution of rabbit polyclonal antibodies raised against His-tagged FtsZ$_{CG}$[20] or GFP (Santa Cruz Biotechnology). Anti-rabbit IgG-AP (Santa Cruz Biotechnology) was used as the secondary antibody at a 1:10,000 dilution.

Microscopy. *C. glutamicum* and *E. coli* cells containing *egfp2*/*gfp* gene constructs or immunofluorescently labeled (see below) were observed in a Nikon E400 fluorescence microscope. Images were taken with a DN100

Table 2. Primers used in this work

Experiment	Primer	Target gene	Nucleotide sequence (5′–3′)
Primer extension	Pext-1	*ftsZ$_{CG}$*	CAATCATGCGGTTGACGGCGTTGACTCCGCCGCCG
	Pext-2	*ftsZ$_{CG}$*	GGACATTTACAGCGGCGTGTCGCTACCCTCAACCT
RACE experiments	raceZ1	*ftsZ$_{CG}$*	CCAATGGTCAGTGCGCCCA
	raceZ2	*ftsZ$_{CG}$*	TCTGCCGAGGCACGTCCAA
	raceZ3	*ftsZ$_{CG}$*	TCCGAGGATCCCCAGTAGATTT
Cloning of the P*ftsZ$_{CG}$* promoter regions	PftsZ1A	P*ftsZ$_{CG}$*	CTA<u>GGATCC</u>AACGCGTTTGCCCACCTCACA (*Bam*HI)
	PftsZ1B	P*ftsZ$_{CG}$*	CTA<u>AGATCT</u>CGCCCACGCCGACGACCTTA (*Bgl*II)
	PftsZ2A	P*ftsZ$_{CG}$*	CTA<u>TGATCA</u>AAGTGCTTCCTGCGGTTATT (*Bcl*I)
	PftsZ2B	P*ftsZ$_{CG}$*	CTA<u>AGATCT</u>CTTTACTTTAGGGTTGTTGAGGTG (*Bgl*II)
	PftsZ3A	P*ftsZ$_{CG}$*	CTA<u>GGATCC</u>GCAGCAGGGCAAAACAT (*Bam*HI)
	PftsZ3B	P*ftsZ$_{CG}$*	CG<u>GGATCC</u>TACAGCAATAACCGCAGG (*Bam*HI)
Cloning of *ftsZ$_{CG}$* without stop codon	ftsZ1	*ftsZ$_{CG}$*	GGAATTC<u>CATATG</u>ACCTCACCGAACAA (*Nde*I)
	ftsZ2	*ftsZ$_{CG}$*	GGAATTC<u>CATATG</u>CTGGAGGAAGCTG (*Nde*I)
Subcloning of *ftsZ$_{CG}$* with stop codon	PgntK	P*gntK*	ACTA<u>GATATC</u>CAGGAAGTATCCGCTCCACG (*Eco*RV)
	Pdiv	P*div*	ACTA<u>GATATC</u>TTGTGGCCTTGAAAG (*Eco*RV)
	ftsZ3	*ftsZ$_{CG}$*	ACGA<u>GATATC</u>TTACTGGAGGAAGCTGGG (*Eco*RV)
Cloning of *ftsZ$_{CG}$* without stop codon into pGFPuv	ftsZ4	*ftsZ$_{CG}$*	CCC<u>AAGCTT</u>ATGACCTCACCGAACAACTA (*Hind*III)
	ftsZ5	*ftsZ$_{CG}$*	GC<u>TCTAGA</u>TACTGGAGGAAGCTGGGTACATCCAGGTCG (*Xba*I)

Fig. 1. Analysis of the promoter regions of *ftsZ* from *Corynebacterium glutamicum*. (**A**) Nucleotide sequence corresponding to the 3′-end of the *ftsQ* gene, the *ftsQ*-*ftsZ* intergenic region, and *ftsZ* 5′-end. The arrows indicate the oligonucleotides used in this study to identify the transcription start points (tsp) by primer extension (dashed arrows) and to clone the three promoter regions of *ftsZ* (full arrows). The numbered squares correspond to the five tsp identified in this study by primer extension or RACE analysis. The putative –10 and –35 boxes for each hypothetical tsp promoter are underlined. (**B**) Primer-extension analysis of *ftsZ_CG*. The arrows indicate the different transcription start points identified using the Pext-2 primer. See text for details. (**C**) Schematic representation of the hypothetical promoters identified in this study (upper panel). DNA fragments (lower panel) containing different promoter regions (P*ftsZ1*, P*ftsZ2*, and P*ftsZ3* alone or combined) were subcloned and their activity evaluated in *E. coli* (using *kan* as the reporter). (**D**) "In vivo" quantification of *ftsZ_CG* promoter strength in *C. glutamicum* transconjugants containing the indicated promoter regions (P*ftsZ*) subcloned into pEGFP derivatives, with *egfp2* serving as the reporter gene. The values are the means of four independent experiments; standard deviations are indicated on the bar tops. (**E**) Western-blot quantification of the amount of FtsZ with respect to the growth of *C. glutamicum* R31. Samples were taken at the optical density (OD$_{600}$) indicated at the top of the image. One μg of total protein from each cell extract was used; the relative intensity of each sample (measured by spectrodensitometry) is indicated at the bottom.

Nikon digital camera and assembled using Corel Draw. Staining with DAPI (4′,6′-diamino-2-phenylindole) and immunofluorescence microscopy were carried out as described previously [7], except that *C. glutamicum* cells were permeabilized overnight at 30ºC with lysozyme at a final concentration of 10 μg/ml. The permeabilized cells were then incubated for 1 h with a 1:1000 dilution of anti-FtsZ$_{CG}$ antiserum. Finally, the samples were incubated overnight at 4ºC with anti-rabbit fluorescein-conjugated secondary antibodies (Santa Cruz Biotechnology) at a 1:10,000 dilution.

For scanning electron microscopy (SEM), exponentially growing *C. glutamicum* cells were collected by centrifugation, fixed for 2 h at room temperature in 2.5% glutaraldehyde in 100 mM cacodylate buffer (pH 7.4), rinsed three times in cacodylate buffer (pH 7.4), and postfixed for 2 h in 1% osmium tetroxide. Cells were washed twice with cacodylate buffer and recovered by filtration through Millipore filters (0.20 μm diameter). The filters containing the cells were passed through an ethanol series of 20, 50, 75, 95, and 100%, critical-point dried, and then coated with a 40-nm-thick layer of gold. The cells were observed by SEM in Jeol JSM-6100 microscope at an accelerating voltage of 20 kV.

Fluorimetry. *C. glutamicum* strains containing pEGFP (P*kan-egfp2*) and pEGNC (carrying promoter-less *egfp2*) (Table 1) were used as positive and negative controls for fluorimetry, respectively. Promoter strength was measured by fluorimetric valuation of the EGFP2 produced, as previously described [29]. Strains containing vector derivatives carrying the pEGFP promoter probe were grown in liquid media. Samples of these cultures were loaded into 96-well microtiter plates and their fluorescence levels measured on a Synergy HT Multi-Detection Microplate Reader Fluorimeter (Bio-Tek Instruments, Inc.). The intrinsic fluorescence level from *C. glutamicum* [pEGNC] was subtracted from all the values obtained. In all cases, the fluorescence level of each sample was divided by the OD$_{600}$ of the sample and normalized to *C. glutamicum* [pEGFP], which was defined as having 100% fluorescence.

Results

Mapping of *ftsZ* mRNA 5′ ends. We identified five *ftsZ* starting transcripts located at nucleotide positions 1170 (tsp1), 971 (tsp2), 925 (tsp3), 780 (tsp4), and 699 (tsp5) (numbered as in database submission Y08964) (Fig. 1A), although it was not clear whether they were produced by transcription initiation or by processing or degradation of mRNA. Transcripts starting at tsp2 and tsp5 corresponded to those previously described [19]. To confirm the RACE results, new primer-extension experiments were carried out using the primer Pext-2 (Table 2; Fig 1A). Again, starting transcripts tsp2, tsp3, tsp4, and tsp5 were obtained (Fig. 1B); however, transcript tsp1 was not found by primer-extension analysis when primer Pext-1 was used (Table 2, Fig. 1A).

Based on these five transcriptional start points, we postulated the presence of five promoters for the *ftsZ*$_{CG}$ gene. These were subsequently investigated by trimming the region located upstream of the structural gene (P*ftsZ* region) into three ~250-bp fragments, P*ftsZ1*, P*ftsZ2*, and P*ftsZ3*, which included the tsp promoters tsp1 (P*ftsZ1*), tsp2, 3 and 4 (P*ftsZ2*) and tsp5 (P*ftsZ3*) (Fig. 1C). Different combinations of these three fragments (Fig. 1C) were cloned into the *E. coli* promoter probe vector pJMFA24 (Table 1). Only *E. coli* transformants containing the pJMFA24 constructions with

the P*ftsZ3* region, combined or not with regions P*ftsZ1* or P*ftsZ2*, directed expression of the *kan* reporter gene present in plasmid pJMFA24 (Fig. 1C). The results of the in vivo quantification of the *ftsZ*$_{CG}$ promoter strength can be summarized as follows (Fig. 1D): (i) higher promoter activity was always obtained when the construct included P*ftsZ3* (tsp5); (ii) fluorescence was proportional to the number of P*ftsZ* regions cloned into the promoter probe vector; (iii) region P*ftsZ1* (tsp1) showed promoter activity in *C. glutamicum,* even when no signal was detected by primer-extension analysis; (iv) all promoter regions were down-regulated during stationary phase, as was confirmed by quantitative Western-blot analysis using anti-FtsZ$_{CG}$ antibodies (Fig. 1E).

Construction of *C. glutamicum* strains carrying a unique complete copy of *ftsZ* under the control of P*gntK*.

The tightly controlled expression of *ftsZ* suggested that small changes in the amount of FtsZ could be extremely detrimental for *C. glutamicum*. In a previous report, we described that the *ftsZ*$_{CG}$ gene (and upstream region), when cloned in different multicopy plasmids (pULMJ880M and pECM2), could not be introduced into *C. glutamicum*; it was therefore assumed that high levels of FtsZ$_{CG}$ result in lethality [40]. Based on the results of the present study, it is clear that those constructs carried *ftsZ* and part of the upstream region but lacked the tsp4 and tsp5 promoters. To clarify whether the lethality of *ftsZ* when cloned in high-copy-number vectors was due to the high copy number or to the partial lack of the *fts* regulatory region, different plasmid constructions were designed. These allowed us to test the lethality of the promoter-less *ftsZ*$_{CG}$ gene under the control of the entire P*ftsZ* or the P*div* promoters [39] when subcloned in the multicopy plasmid pECM2. P*div* is considered to be a strong promoter for *C. glutamicum* and has been shown to have 5-fold higher promoter activity than the P*kan* promoter from Tn*5* (Letek et al., submitted). No transconjugants were obtained using pEGZ (P*ftsZ123-ftsZ*$_{CG}$), pEAG7 (P*div-ftsZ*$_{CG}$), or pEAG7E (P*div-ftsZ*$_{CG}$-*egfp2*) (Table 1), in contrast to the control experiment in which a high number of transconjugant colonies were produced when the donor strain *E. coli* S17-1 was transformed with pEGZ123 (P*ftsZ123-egfp2*) or pEAG6 (P*div-egfp2*) (Table 1).

In order to control expression of the *ftsZ* gene in *C. glutamicum*, and due to the lack of low-copy-number vectors for *C. glutamicum*, the chromosomal copy of *ftsZ* was disrupted and replaced by *ftsZ* under the control of the *gntK* promoter (P*gntK*) from *C. glutamicum*. This promoter was chosen because it is catabolite-regulated in *C. glutamicum* [29]. The resulting strain [*C. glutamicum* KF (Table 1)] had a partial, non-functional *ftsZ* gene in the original chromosomal position and a complete copy of *ftsZ* under the control of P*gntK*. When grown in MMC medium supplemented with 2% glu-

cose, *C. glutamicum* KF behaved like the wild-type strain whereas in MMC supplemented with 2% fructose or 4% sucrose (repressive conditions) the cells acquired a filamentous shape, indicative of inhibition of cell division (Fig. 2A). In contrast, in MMC supplemented with 1% gluconate, the cell diameter increased significantly (Fig. 2A).

Quantitative Western-blot analysis using anti-FtsZ$_{CG}$ antibodies obtained previously [20] confirmed the variations in FtsZ levels in *C. glutamicum* KF grown in the presence of different carbon sources (Fig. 2B). The amount of FtsZ was 2.6-fold higher in cells grown in the presence of 1% gluconate (Fig. 2B, lane 2) than in those grown in the presence of 2% glucose or in the wild-type strain (Fig. 2B, lane 1). A 4-fold reduction of the FtsZ level was obtained in cells cultured in the presence of 2% fructose (Fig. 2B, lane 4), while in the presence of 4% sucrose the reduction was even higher (Fig. 2B, lane 5). These positive results following overexpression of *ftsZ* led us to increase as much as possible the concentration of its gene product in *C. glutamicum.*

Multicopy plasmids carrying *ftsZ* under P*gntK* can be introduced into *C. glutamicum.* The homologous overexpression of *ftsZ* genes has been studied in several species of bacteria, including *E. coli, Neisseria gonorrhoeae* [43], *Halobacterium salinarum* [34], *Mycobacterium tuberculosis* [8], and *C. glutamicum* [40]. In *E. coli,* a two- to seven-fold increase in the level of the FtsZ protein was shown to increase the number of septa near the cell poles, producing minicells. In addition, an increase in the level of FtsZ beyond this range resulted in the complete inhibition of cell division [55]. In *N. gonorrhoeae,* higher amounts of FtsZ resulted in abnormal cell division, characterized by the presence of multiple and atypically arranged cell-division septa. In *H. salinarium, M. tuberculosis,* and *C. glutamicum,* the unregulated expression of *ftsZ* was lethal to the cells.

The controlled overexpression of FtsZ in *C. glutamicum* was achieved by constructing a bifunctional *E. coli*–corynebacteria mobilizable plasmid that carried the *ftsZ* gene under the control of promoter P*gntK* and fused, or not, to *egfp2,* yielding plasmids pEKFG and pEKF, respectively (Table 1). Mobilization of these plasmids into *C. glutamicum* by conjugation resulted in transconjugants that expressed a wild-type morphology in MMC + 4% sucrose (higher repression; Fig. 2C), despite the high copy number of the plasmid. However, the transconjugants were unable to grow in MMC supplemented with 1% gluconate or 2% glucose and showed slower growth and reduced cell viability in MMC + 2% fructose compared with *C. glutamicum* [pECM2] (Fig. 2D,E). The growth kinetics and viability of *C. glutamicum* [pEKFG] grown in MMC + 4% sucrose were similar to the wild-type strain and the cells showed a clearly visible fluorescent band at mid-cell, supporting the functionality of FtsZ-EGFP2 in

this strain (Fig. 2C). However, in MMC + 2% fructose (higher repressor conditions), the transconjugants showed a delayed growth and reduced cell viability when compared to *C. glutamicum* [pECM2] (Fig. 2D,E), in which growth kinetics and viability were similar to the wild-type strain. Furthermore, *C. glutamicum* [pEKFG] was unable to grow in MMC supplemented with 1% gluconate or 2% glucose (lower repression conditions). Quantitative Western-blot analysis confirmed the nearly 5-fold increase in the amount of FtsZ in *C. glutamicum* [pEKF] grown in MMC + 2% fructose (Fig. 2B, lane 6), whereas in MMC + 4% sucrose the FtsZ concentration was similar to that of the wild-type strain (Fig. 2B, lane 7).

When *C. glutamicum* [pEKFG] was grown in MMC + 2% fructose, the localization of FtsZ-EGFP2 was highly variable, but it could be generally described as forming spirals or tangles throughout the cell (Fig. 2C). Identical results were obtained with *C. glutamicum* [pEKF] (P*gntK-ftsZ*) when the native FtsZ$_{CG}$ was detected by immunofluorescence (IFL). In contrast, under high repression conditions (MMC + 4% Suc), FtsZ$_{CG}$-EGFP2 localized only at mid-cell. The localization of FtsZ, as determined by immunofluorescence detection, was essentially the same when the strain containing pEKF was cultured under the same nutritional conditions (Fig. 2C).

In contrast to the typical nucleoid segregation and wild-type morphology evident in *C. glutamicum* [pECM2] (Fig. 3A), nucleoid localization of *C. glutamicum* [pEKF] grown in MMC + 2% fructose was distorted due to overexpression of FtsZ, and most of the swollen cells presented one large nucleoid in the widest part of the cell (Fig. 3B). SEM revealed that these aberrant cells showed patches and small invaginations along their surfaces, suggesting several attempts of nonetheless failed cell division (Fig. 3C).

Expression of FtsZ$_{CG}$-GFP in *E. coli.* In strain *E. coli* TOP10 [pZGFP], overexpression of FtsZ$_{CG}$-GFP under the control of P*lac* resulted, when induced by IPTG, in an inhibition of cell division and the formation of long filaments (Fig. 4B), as previously described for the overproduction of FtsZ by *Rhizobium* [33], *Bacillus* [2], *Mycoplasma* [54], *Neisseria* [43], and *Corynebacterium* [19]. The filaments contained several discrete fluorescent dots located along the entire cell. This pattern contrasted widely with that characteristic of the wild-type morphology and with the lack of localization of GFP expressed in *E. coli* TOP10 [pGFPuv] (Fig. 4A). Fused FtsZ$_{CG}$-GFP was readily detected in soluble fractions by Western blotting with anti-GFP antibodies (data no shown), suggesting that the fluorescent aggregates represent multiple cell-division sites or multiple Z-rings. These observations suggested that the relatively high expression of FtsZ$_{CG}$-GFP interfered with FtsZ$_{EC}$, blocking cell division. However, when strain *E. coli* HB101, transformed with plasmid pZGFP and grown in the presence of IPTG, was similarly examined,
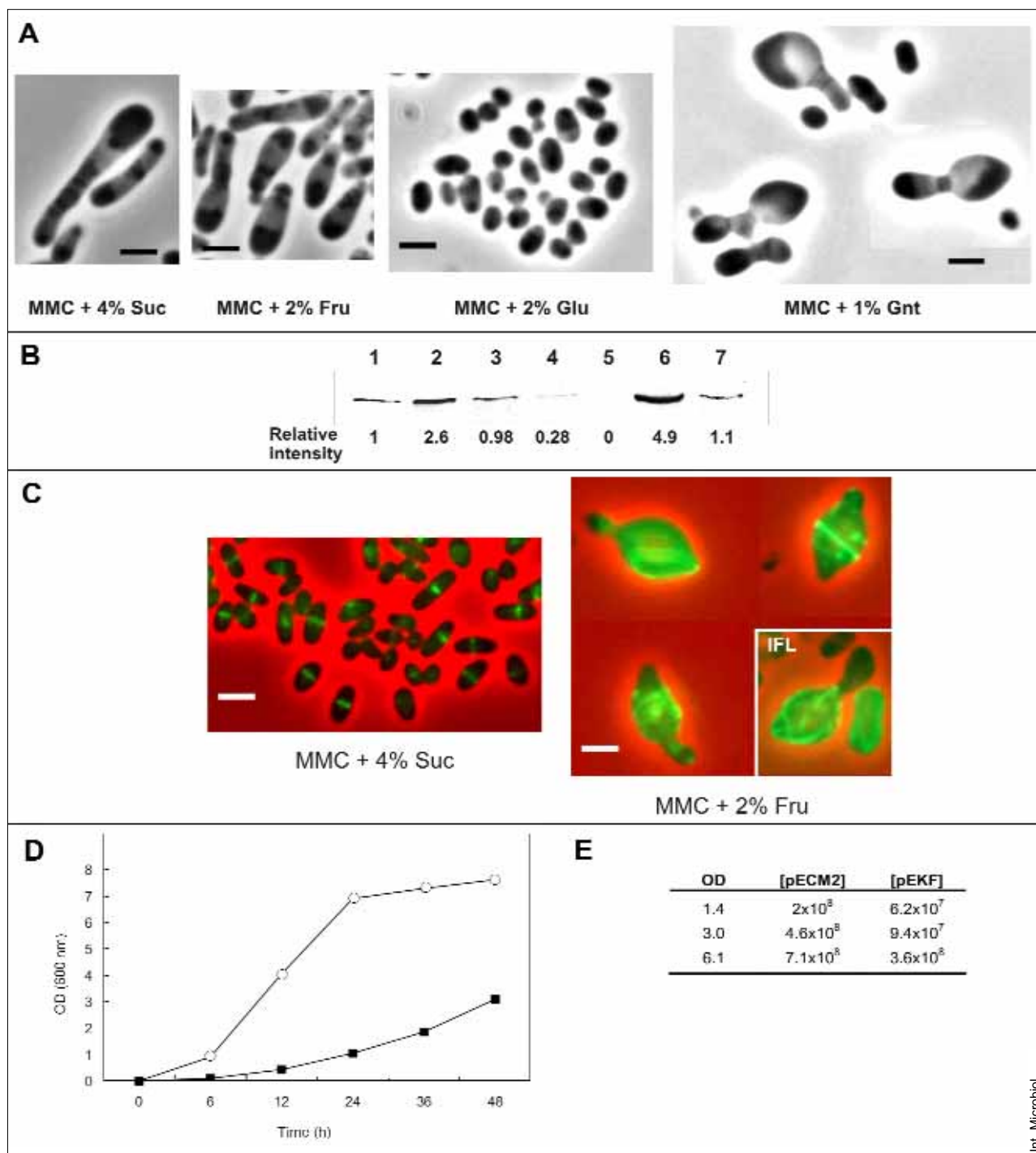
Fig. 2. Controlled expression of *ftsZ* in *Corynebacterium glutamicum* carrying a functional copy of P*gntK-ftsZ* in the chromosome (strain KF) or in a high-copy-number plasmid (strains pEKF or pEKFG, respectively). (**A**) Phase-contrast microscopy of *C. glutamicum* KF grown in MMC in the presence of different carbon sources. Bars represent 1 μm. (**B**) Western-blot quantification of FtsZ in exponentially growing (OD_{600} = 2.0) *C. glutamicum* R31, KF, or [pEKF] cultured in MMC with the indicated carbon source. One μg of total protein from each cell extract was used; the relative intensity of each sample (measured by spectrodensitometry) is indicated at the bottom. Lane 1, *C. glutamicum* R31 grown in 4% sucrose (4% Suc); lane 2, *C. glutamicum* KF in 1% gluconate (1% Gnt); lane 3, *C. glutamicum* KF in 2% glucose (2% Glu); lane 4, *C. glutamicum* KF in 2% fructose (2% Fru); lane 5, *C. glutamicum* KF in 4% Suc; lane 6, *C. glutamicum* [pEKF] in 2% Fru; lane 7, *C. glutamicum* [pEKF] in 4% Suc. (**C**) Expression of *ftsZ* under the control of P*gntK*. Overlays combining phase-contrast and fluorescence microscopy of *C. glutamicum* [pEKFG] (P*gntK-ftsZ-egfp2*). Bars represent 1 μm. (**D**) Growth kinetics of *C. glutamicum* [pECM2] (open circles) and *C. glutamicum* [pEKF] (closed squares) when cultured in MMC + 4% Suc. (**E**) Viable cells of *C. glutamicum* [pECM2] and [pEKF] strains grown on MMC + 4% Suc. Note that cell viability of *C. glutamicum* [pEKF] is reduced.
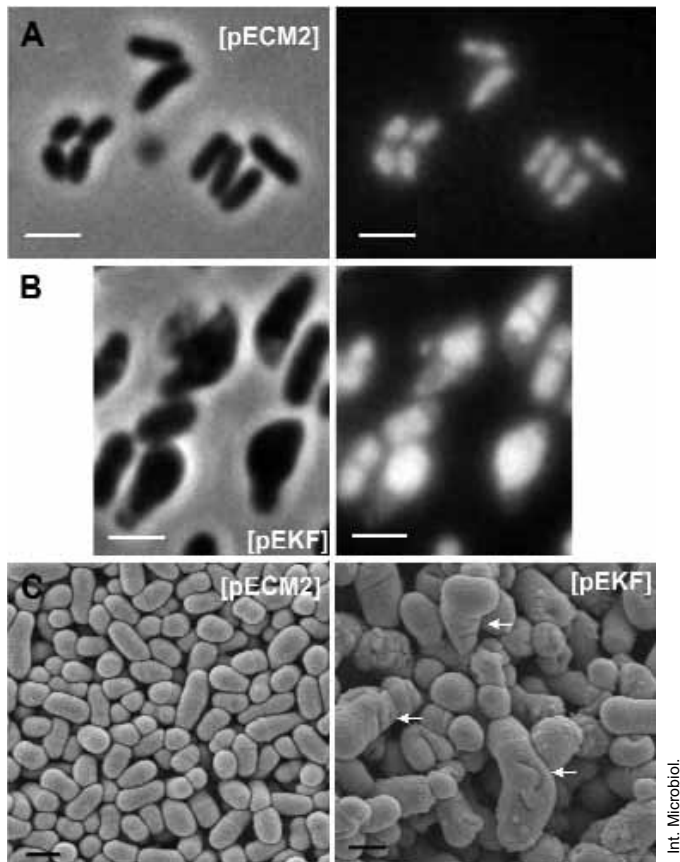
Fig. 3. Nucleoid staining and scanning electron microscopy (SEM) of *Corynebacterium glutamicum* strains. DNA distribution was visualized by phase-contrast (left panels) and DAPI staining (right panels) in: (**A**) *C. glutamicum* [pECM2] and (**B**) *C. glutamicum* [pEKF]. Both strains were grown in MMC + 2% Fru. Bars represent 1 µm. (**C**) SEM of *C. glutamicum* [pECM2] (left) and *C. glutamicum* [pEKF] (right) grown in both cases in MMC + 2% Fru. Arrows showed invaginations of patches, indicative of failed division events.

filamentous cells containing different fluorescent structures were observed (Fig. 4C). The latter consisted of single-helix-strand-like structures or of FtsZ$_{CG}$-GFP localized over the cell surface. In the absence of IPTG, the cells were morphologically wild-type, and no fluorescence was detected by fluorescence microscopy. Figure 4C shows the diverse localization patterns of FtsZ$_{CG}$-GFPuv in this strain.

Discussion

Corynebacterium glutamicum is a rod-shaped actinomycete with a distinctly polar cell-elongation pattern [6] and lacking the bacterial actin homolog MreB (or equivalent genes). Cell division of this microorganism also differs since there are no homologs to the cell-division genes *ftsL* or *ftsN* (Table 3), which are essential for other bacteria [15]. However, perhaps the most intriguing finding is the total lack of positive or neg-
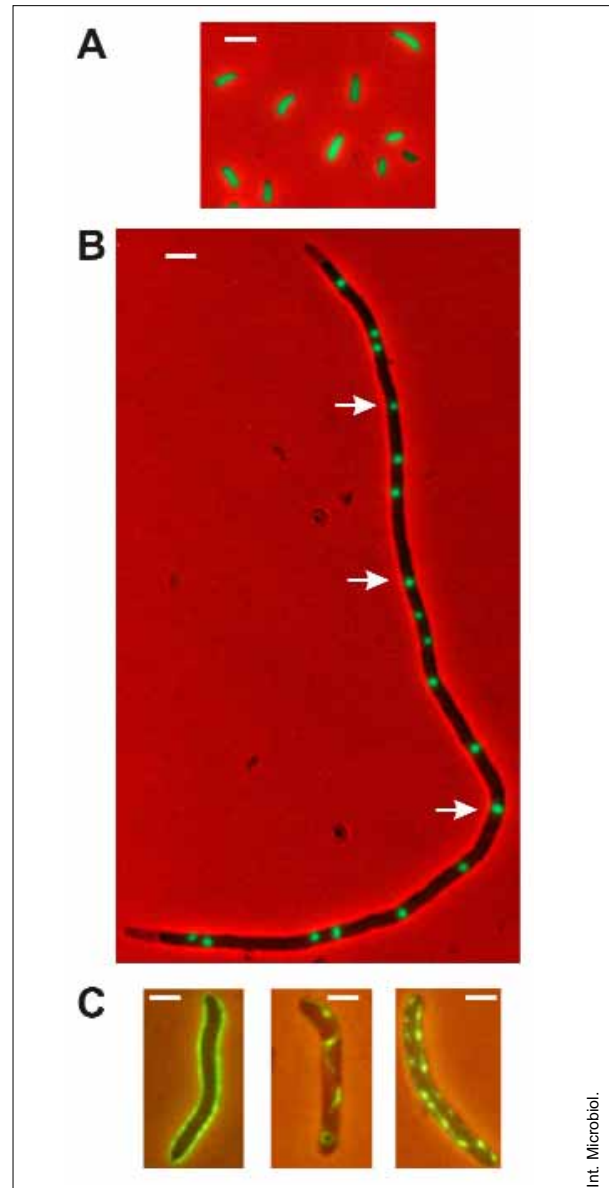

Fig. 4. Localization of *FtsZ$_{CG}$*-GFPuv in *Escherichia coli*. Overlays combining phase-contrast and fluorescence microscopy of *E. coli* TOP10 transformed with (**A**) the control plasmid pGFPuv, or (**B**) the plasmid pZGFP (*FtsZ$_{CG}$*-GFPuv). (**C**) *E. coli* HB101 transformed with pZGFP. Bars represent 1 µm.

ative regulators of cell division in *C. glutamicum* (Table 3), as is the case in other actinomycetes [10]. Specifically, in this microorganism there are no homologs to *ezrA*, *ftsA*, *min*, *noc*, *slmA*, *sulA*, *zipA* or *zapA*. Moreover, in actinomycetes DivIVA is involved in polar cell growth, rather than acting as a regulator of FtsZ, as is the case in *B. subtilis* [11,39]. In addition, *C. glutamicum* is deficient in a nucleoid occlusion system, which in other bacteria is a temporal and spatial regulation factor of FtsZ assembly [40]. It has been suggested that changes in the membrane composition at future cell-division sites contributes to the

Table 3. Genes related to cell division and cell growth in the *Escherichia coli*, *Bacillus subtilis* and *Corynebacterium glutamicum* genomes. The functions of the codified proteins were recently reviewed [15]

Gene name	Escherichia coli	Bacillus subtilis	Corynebacterium glutamicum
amiC	(b2817)	(BSU35620)	(cg3424)
divIVA	–	(BSU15420)	(cg2361)
ezrA	–	(BSU29610)	–
ftsA	(b0094)	(BSU15280)	–
ftsB	(b2748)	–	(cg1112)
ftsE	(b3463)	(BSU35260)	(cg0914)
ftsI	(b0084)	(BSU15170)	(cg2375)
ftsK	(b0890)	ytpT (BSU29800) spoIIIE (BSU16800)	(cg2158)
ftsL	(b0083)	(BSU15150)	–
ftsN	(b3933)	–	–
ftsQ	(b0093)	–	(cg2367)
ftsW	(b0089)	ftsW (BSU14850) spoVE (BSU15210)	(cg2370)
ftsX	(b3462)	(BSU35250)	(cg0915)
ftsZ	(b0095)	(BSU15290)	(cg2366)
minC	(b1176)	(BSU28000)	–
minD	(b1175)	(BSU27990)	–
minE	(b1174)	–	–
mreB	(b3251)	mreBH (BSU14470) mreB (BSU28030) mbl (BSU36410)	–
mreC	(b3250)	(BSU28020)	–
mreD	(b3249)	(BSU28010)	–
noc	–	(BSU40990)	–
rodA	(b0634)	(BSU38120)	(cg0061)
sepF	–	(BSU15390)	(cg2363)
smlA	(b3641)	–	–
sulA	(b0958)	–	–
zapA	(b2910)	–	–
zipA	(b2412)	–	–

regulation of FtsZ assembly in microorganisms that lack systems such as nucleoid occlusion [32]. Our results suggested that only the promoter present in P*ftsZ3* (corresponding to tsp5) was functional in *E. coli*, a frequent circumstance described for corynebacterial promoters [35,38]. The hypothetical –10 and –35 boxes from the five *ftsZ* promoters are indicated in Fig. 1A, although in certain cases no consensus motifs for the described corynebacterial promoters [38] were found.

Taking into account the many promoters that control the expression of *ftsZ* (Fig. 1A), its transcriptional regulation is most likely essential to the temporal regulation of cell divi-

sion. The existence of different promoter regions for *ftsZ* was previously described for *E. coli*, in which at least two promoters lie in the upstream *ftsA* gene [12,14], as well as in *S. coelicolor* [13] and *M. tuberculosis* [42]. The FtsZ promoter regions were active only during exponential growth phase and were down-regulated during stationary phase (Fig. 1D). Therefore, an as-yet-unknown factor should direct cell division in *C. glutamicum* in response to environmental conditions, as was suggested previously in other bacteria [1,50].

It is well-established that cellular changes in FtsZ levels directly influence bacterial cell morphology and viability. In

a previous report, we described the morphological effects produced in *C. glutamicum* by lowering the cellular concentration of FtsZ, although FtsZ overexpression was not obtained [40]. In this study, we showed that the introduction of multiple copies of *ftsZ*$_{CG}$, either under the control of the gene's own promoter region or an endogenous strong promoter (P*div*), was unsuccessful and most likely lethal, as no transconjugants were ever obtained. Therefore, in order to analyze the effect of controlled expression, *ftsZ*$_{CG}$ was expressed under the catabolite-regulated gluconate promoter (P*gntK*) from *C. glutamicum* [29] as a single copy on the chromosome (*C. glutamicum* KF). In this strain, FtsZ expression increased 2.6-fold in the absence of repression conditions (with gluconate), and decreased when the strain was grown in the presence of fructose or sucrose (Fig. 2B). Therefore, *C. glutamicum* KF can be considered a model strain to study the phenotypic effects produced by alteration of FtsZ levels, changing only the nutritional conditions.

Catabolite-regulated expression of *ftsZ* opened up the way to selecting *C. glutamicum* strains carrying *ftsZ* in high copy number. Accordingly, the *ftsZ*$_{CG}$ gene could be introduced, either alone (pEKF) or fused to the *egfp2* gene (pEKFG), into *C. glutamicum* under repressive conditions. When those cells were grown under non-repressive conditions, clear alterations of cell diameter, cell morphology, and nucleoid segregation occurred (Figs. 2C, 3B). These changes differed from the typical asymmetric cell observed in *E. coli* or *B. subtilis* overexpressing FtsZ [55,56]. When FtsZ was overexpressed in *C. glutamicum*, it localized in spindles or tangles throughout the cell (Fig. 2C). Thus, it may have been that FtsZ was unable to carry out its normal function in cell division because of its anarchic pattern of localization. In addition, the altered morphology suggested that the normal distribution of FtsZ plays a role in the maintenance of cell diameter in *C. glutamicum*.

In *E. coli*, the overexpression of *ftsZ*$_{CG}$ led to a filamentous phenotype and the fused FtsZ$_{CG}$-GFP localized in multiple septa (Fig. 4B). There are several descriptions of the localization of heterologous FtsZ-GFP in *E. coli*, and in all cases it was concluded that, as long as the level of heterologous FtsZ-GFP is the same or lower than that of FtsZ$_{EC}$, a high percentage of cells will express the fused protein as a single or double fluorescent band at mid-cell [30,43]. When the levels of heterologous FtsZ-GFP are above those of FtsZ$_{EC}$, the cells show spaced bands (multiple FtsZ rings), aggregates that most likely are genuine structures and not inclusion bodies, as well as spiral tubules [30] and double-helix-like strands [42]. Some of these structures were observed when FtsZ$_{CG}$-GFP was expressed in different *E. coli* strains, although the exact localization of the fused protein changed depending on the *E. coli* strain used [43]. Nonetheless, the observed accumulation of FtsZ$_{CG}$-GFP

throughout *E. coli* HB101 cells has not been reported previously. However, the biological significance and the potential role of the previously described spiral tubules or the equally spaced dots/bands widely distributed over the cell—as found in this study—remain to be determined. The formation of ring-like structures at mid-cell or the generation of spirals and double-helix-like structures shows the ability of FtsZ to alternate between forming a localized ring at the prospective division site and becoming more randomly dispersed [43], suggesting that FtsZ$_{CG}$ is able to co-polymerize in *E. coli* when FtsZ$_{EC}$ directs the insertion of new peptidoglycan into portions of the lateral wall [52].

The transcriptional regulation of *ftsZ* plays a crucial role in the maintenance of the correct cell shape in *C. glutamicum*. The strains obtained in this work can be considered as good tools to study or identify new proteins involved in the regulation of cell division in this actinomycete, which presents a distinct model of cell division and cell growth.

References

1. Ahmer BM, van Reeuwijk J, Timmers CD, Valentine PJ, Heffron F (1998) *Salmonella typhimurium* encodes an SdiA homolog, a putative quorum sensor of the LuxR family, that regulates genes on the virulence plasmid. J Bacteriol 180:1185-1193

2. Beall B, Lowe M, Lutkenhaus J (1988) Cloning and characterization of *Bacillus subtilis* homologs of *Escherichia coli* cell division genes *ftsZ* and *ftsA*. J Bacteriol 170:4855-4864

3. Bi E, Lutkenhaus J (1991) FtsZ ring structure associated with division in *Escherichia coli*. Nature 354:161-164

4. Bradford MM (1976) A rapid and sensitive method for the quantitation of microgram quantities of protein utilizing the principle of protein-dye binding. Anal Biochem 72:248-254

5. Bramhill D, Thompson CM (1994) GTP-dependent polymerization of *Escherichia coli* FtsZ protein to form tubules. Proc Natl Acad Sci USA 91:5813-5817

6. Daniel RA, Errington J (2003) Control of cell morphogenesis in bacteria: two distinct ways to make a rod-shaped cell. Cell 113:767-776

7. Daniel RA, Harry EJ, Errington J (2000) Role of penicillin-binding protein PBP 2B in assembly and functioning of the division machinery of *Bacillus subtilis*. Mol Microbiol 35:299-311

8. Dziadek J, Madiraju MVVS, Rutherford SA, Atkinson MAL, Rajagopalan M (2002) Physiological consequences associated with overproduction of *Mycobacterium tuberculosis* FtsZ in mycobacterial hosts. Microbiology 148:961-971

9. Errington J, Daniel RA, Scheffers DJ (2003) Cytokinesis in bacteria. Microbiol Mol Biol Rev 67:52-65

10. Flärdh K (2003) Growth polarity and cell division in *Streptomyces*. Curr Opin Microbiol 6:564-571

11. Flärdh K (2003) Essential role of DivIVA in polar growth and morphogenesis in *Streptomyces coelicolor* A3(2). Mol Microbiol 49:1523-1536

12. Flärdh K, Garrido T, Vicente M (1997) Contribution of individual pro-

moters in the *ddlB-ftsZ* region to the transcription of the essential cell-division gene *ftsZ* in *Escherichia coli*. Mol Microbiol 24:927-936

13. Flärdh K, Leibovitz E, Buttner MJ, Chater KF (2000) Generation of a non-sporulating strain of *Streptomyces coelicolor* A3(2) by the manipulation of a developmentally controlled *ftsZ* promoter. Mol Microbiol 38:737-749

14. Garrido T, Sanchez M, Palacios P, Aldea M, Vicente M (1993) Transcription of *ftsZ* oscillates during the cell cycle of *Escherichia coli*. EMBO J 12:3957-3965

15. Goehring NW, Beckwith J (2005) Diverse paths to midcell: assembly of the bacterial cell division machinery. Curr Biol 15:R514-R526

16. Gonzy-Treboul G, Karmazyn-Campelli C, Stragier P (1992) Developmental regulation of transcription of the *Bacillus subtilis ftsAZ* operon. J Mol Biol 224:967-979

17. Guerrero R, Berlanga M (2007) The hidden side of the prokaryotic cell: rediscovering the microbial world. Int Microbiol 10:157-168

18. Hanahan D (1983) Studies on transformation of *Escherichia coli* with plasmids. J Mol Biol 166:557-580

19. Honrubia MP, Fernández FJ, Gil JA (1998) Identification, characterization, and chromosomal organization of the *ftsZ* gene from *Brevibacterium lactofermentum*. Mol Gen Genet 259:97-104

20. Honrubia-Marcos MP, Ramos A, Gil JA (2005) Overexpression of the *ftsZ* gene from *Corynebacterium glutamicum* (*Brevibacterium lactofermentum*) in *Escherichia coli*. Can J Microbiol 51:85-89

21. Huang Q, Tonge PJ, Slayden RA, Kirikae T, Ojima I (2007) FtsZ: a novel target for tuberculosis drug discovery. Curr Top Med Chem 7:527-543

22. Jäger W, Schafer A, Pühler A, Labes G, Wohlleben W (1992) Expression of the *Bacillus subtilis sacB* gene leads to sucrose sensitivity in the gram-positive bacterium *Corynebacterium glutamicum* but not in *Streptomyces lividans*. J Bacteriol 174:5462-5465

23. Kainz M, Roberts J (1992) Structure of transcription elongation complexes in vivo. Science 255:838-841

24. Kaneko H, Sakaguchi K (1979) Fusion of protoplasts and genetic recombination of *Brevibacterium flavum*. Agric Biol Chem 43:1007-1013

25. Kelly AJ, Sackett MJ, Din N, Quardokus E, Brun YV (1998) Cell cycle-dependent transcriptional and proteolytic regulation of FtsZ in *Caulobacter*. Genes Dev 12:880-893

26. Kieser T, Bibb MJ, Buttner MJ, Chater KF, Hopwood DA (eds) (2000) Practical *Streptomyces* genetics. The John Innes Foundation, Norwich, UK

27. Laemmli UK (1970) Cleavage of structural proteins during the assembly of the head of bacteriophage T4. Nature 227:680-685

28. Letek M, Ordoñez E, Fernández-Natal I, Gil JA, Mateos LM (2006) Identification of the emerging skin pathogen *Corynebacterium amycolatum* using PCR-amplification of the essential *divIVA* gene as a target. FEMS Microbiol Lett 265:256-263

29. Letek M, Valbuena N, Ramos A, Ordoñez E, Gil JA, Mateos LM (2006) Characterization and use of catabolite-repressed promoters from gluconate genes in *Corynebacterium glutamicum*. J Bacteriol 188:409-423

30. Ma X, Ehrhardt DW, Margolin W (1996) Colocalization of cell division proteins FtsZ and FtsA to cytoskeletal structures in living *Escherichia coli* cells by using green fluorescent protein. Proc Natl Acad Sci USA 93:12998-13003

31. Margolin W (2000) Themes and variations in prokaryotic cell division. FEMS Microbiol Rev 24:531-548

32. Margolin W (2005) FtsZ and the division of prokaryotic cells and organelles. Nat Rev Mol Cell Biol 6:862-871

33. Margolin W, Corbo JC, Long SR (1991) Cloning and characterization of a *Rhizobium meliloti* homolog of the *Escherichia coli* cell division gene *ftsZ*. J Bacteriol 173:5822-5830

34. Margolin W, Wang R, Kumar M (1996) Isolation of an *ftsZ* homolog from the archaebacterium *Halobacterium salinarium*: implications for the evolution of FtsZ and tubulin. J Bacteriol 178:1320-1327

35. Mateos LM, Pisabarro A, Pátek M, Malumbres M, Guerrero C, Eikmanns BJ, Sahm H, Martín JF (1994) Transcriptional analysis and regulatory signals of the *hom-thrB* cluster of *Brevibacterium lactofermentum*. J Bacteriol 176:7362-7371

36. Mateos LM, Schäfer A, Kalinowski J, Martín JF, Pühler A (1996) Integration of narrow-host-range vectors from *Escherichia coli* into the genomes of amino acid-producing corynebacteria after intergeneric conjugation. J Bacteriol 178:5768-5775

37. Mateos LM, Ordóñez E, Letek M, Gil JA (2006) *Corynebacterium glutamicum* as a model bacterium for bioremediation of arsenic. Int Microbiol 9:207-215

38. Patek M, Nesvera J, Guyonvarch A, Reyes O, Leblon G (2003) Promoters of *Corynebacterium glutamicum*. J Biotechnol 104:311-323

39. Ramos A, Honrubia MP, Valbuena N, Vaquera J, Mateos LM, Gil JA (2003) Involvement of DivIVA in the morphology of the rod-shaped actinomycete *Brevibacterium lactofermentum*. Microbiology 149:3531-3542

40. Ramos A, Letek M, Campelo AB, Vaquera J, Mateos LM, Gil JA (2005) Altered morphology produced by *ftsZ* expression in *Corynebacterium glutamicum* ATCC 13869. Microbiology 151:2563-2572

41. Rothfield L, Taghbalout A, Shih YL (2005) Spatial control of bacterial division-site placement. Nat Rev Microbiol 3:959-968

42. Roy S, Ajitkumar P (2005) Transcriptional analysis of the principal cell division gene, *ftsZ*, of *Mycobacterium tuberculosis*. J Bacteriol 187:2540-2550

43. Salimnia H, Radia A, Bernatchez S, Beveridge TJ, Dillon JR (2000) Characterization of the *ftsZ* cell division gene of *Neisseria gonorrhoeae*: expression in *Escherichia coli* and *N. gonorrhoeae*. Arch Microbiol 173:10-20

44. Sanger F, Nicklen S, Coulson AR (1977) DNA sequencing with chain-terminating inhibitors. Proc Natl Acad Sci USA 74:5463-5467

45. Santamaria RI, Gil JA, Martin JF (1985) High-frequency transformation of *Brevibacterium lactofermentum* protoplasts by plasmid DNA. J Bacteriol 162:463-467

46. Schäfer A, Kalinowski J, Simon R, Seep-Feldhaus AH, Puhler A (1990) High-frequency conjugal plasmid transfer from gram-negative *Escherichia coli* to various gram-positive coryneform bacteria. J Bacteriol 172:1663-1666

47. Schafer A, Tauch A, Jager W, Kalinowski J, Thierbach G, Puhler A (1994) Small mobilizable multi-purpose cloning vectors derived from the *Escherichia coli* plasmids pK18 and pK19: selection of defined deletions in the chromosome of *Corynebacterium glutamicum*. Gene 145:69-73

48. Shih YL, Rothfield L (2006) The bacterial cytoskeleton. Microbiol Mol Biol Rev 70:729-754

49. Siemering K, Golbik R, Sever R, Haseloff J (1996) Mutations that suppress the thermosensitivity of green fluorescent protein. Curr Biol 6:1653-1663

50. Slayden RA, Knudson DL, Belisle JT (2006) Identification of cell cycle regulators in *Mycobacterium tuberculosis* by inhibition of septum formation and global transcriptional analysis. Microbiology 152:1789-1797

51. Tauch A, Kaiser O, Hain T et al (2005) Complete genome sequence and analysis of the multiresistant nosocomial pathogen *Corynebacterium jeikeium* K411, a lipid-requiring bacterium of the human skin flora. J Bacteriol 187:4671-4682

52. Varma A, de Pedro MA, Young KD (2007) FtsZ directs a second mode of peptidoglycan synthesis in *Escherichia coli*. J Bacteriol 189:5692-5704

53. Wang J, Galgoci A, Kodali S, et al. (2003) Discovery of a small molecule that inhibits cell division by blocking FtsZ, a novel therapeutic target of antibiotics. J Biol Chem 278:44424-44428

54. Wang X, Lutkenhaus J (1996) Characterization of the *ftsZ* gene from *Mycoplasma pulmonis*, an organism lacking a cell wall. J Bacteriol 178:2314-2319

55. Ward JE Jr., Lutkenhaus J (1985) Overproduction of FtsZ induces mini-cell formation in *E. coli*. Cell 42:941-949

56. Weart RB, Levin PA (2003) Growth rate-dependent regulation of medial FtsZ ring formation. J Bacteriol 185:2826-2834

57. Woldringh CL, Mulder E, Huls PG, Vischer N (1991) Toporegulation of bacterial division according to the nucleoid occlusion model. Res Microbiol 142:309-320